Molecular characterization of *Plasmodium falciparum* *S*-adenosylmethionine synthetase

Peter K. CHIANG*†[1], Margaret E. CHAMBERLIN†, Diarmuid NICHOLSON‡, Sandrine SOUBES§, Xin-zhuan SU§, Gangadharan SUBRAMANIAN§, David E. LANAR*, Sean T. PRIGGE*, John P. SCOVILL*, Louis H. MILLER§ and Janice Y. CHOU†

*Walter Reed Army Institute of Research, Washington, DC 20307-5100, U.S.A., †National Institute of Child Health and Human Development, National Institutes of Health, Bethesda, MD 20892, U.S.A., ‡Walter Reed Army Medical Center, Washington, DC, U.S.A., and §National Institute of Allergy and Infectious Diseases, National Institutes of Health, Bethesda, MD 20892, U.S.A.

S-Adenosylmethionine (AdoMet) synthetase (SAMS: EC 2.5.1.6) catalyses the formation of AdoMet from methionine and ATP. We have cloned a gene for *Plasmodium falciparum* AdoMet synthetase (*PfSAMS*) (GenBank accession no. AF097923), consisting of 1209 base pairs with no introns. The gene encodes a polypeptide (PfSAMS) of 402 amino acids with a molecular mass of 44 844 Da, and has an overall base composition of 67 % A + T. *PfSAMS* is probably a single copy gene, and was mapped to chromosome 9. The PfSAMS protein is highly homologous to all other SAMS, including a conserved motif for the phosphate-binding P-loop, HGGGAFSGKD, and the signature hexapeptide, GAGDQG. All the active-site amino acids for the binding of ADP, P_i and metal ions are similarly preserved, matching entirely those of human hepatic SAMS and *Escherichia coli* SAMS. Molecular modelling of PfSAMS guided by the X-ray crystal structure of *E. coli* SAMS indicates that PfSAMS binds ATP/Mg^{2+} in a manner similar to that seen in the *E. coli* SAMS structure. However, the PfSAMS model shows that it can not form tetramers as does *E. coli* SAMS, and is probably a dimer instead. There was a differential sensitivity towards the inhibition by cycloleucine between the expressed PfSAMS and the human hepatic SAMS with K_i values of 17 and 10 mM, respectively. Based on phylogenetic analysis using protein parsimony and neighbour-joining algorithms, the malarial PfSAMS is closely related to SAMS of other protozoans and plants.

Key words: Phylogeny, cycloleucine, modelling, chromosome.

INTRODUCTION

S-Adenosylmethionine (AdoMet) synthetase (ATP: L-methionine *S*-adenosyltransferase, EC 2.5.1.6) catalyses the formation of AdoMet from methionine and ATP [1–4]. AdoMet is the major donor of a methyl group for methylation reactions, and is the source of a propylamino moiety for polyamine biosynthesis. Perturbation of the methylation reactions in diverse organisms can lead to disruptions in a variety of biochemical and biological functions, including potent anti-infective activities [4–7]. The enzymic reaction of AdoMet synthetase (SAMS) consists of the following:

$$\text{ATP} + \text{L-methionine} \rightarrow \text{AdoMet} + \text{PP}_i + \text{P}_i$$

The overall reaction of SAMS is composed of two sequential steps, AdoMet formation and the subsequent triphosphatase reaction that hydrolyses triphosphate to pyrophosphate and orthophosphate in the presence of Mg^{2+} and K^+. Thus, this enzyme is an interesting candidate for the development of inhibitors based on methionine analogues or ATP analogues. In yeast and in mammals, there are at least two genes encoding isoenzymes or homologous subunits of SAMS [2,8–11]. In the yeast, the two SAMS genes are *SAM1* and *SAM2* [9], while in *Escherichia* they are *metK* and *metX* [10]. The two human genes are *MAT1A* and *MAT2A*, encoding the α1 and α2 subunits of MAT I/III and MATII, respectively [8]. The *SAMS* gene from *Plasmodium falciparum*, a protozoan parasite that causes malaria with greatest morbidity and mortality, has not been described yet.

Malaria research is in a phase of genetic discovery and genomic characterization, an endeavour that should yield information essential to the understanding of parasitism and its pathogenesis [12,13]. The genomic approach will generate a database for the population genetics of malaria parasites and contribute to the development of antimalarial paradigms [14]. Since methylation of macromolecules by SAMS has been implicated in the development of organisms or diseases [5,6,15,16], and inhibitors of methylation have been shown to exert antimalarial activity *in vitro* and *in vivo* [6,17–20], we describe here a gene coding for SAMS from *Plasmodium falciparum* (*PfSAMS*) (GenBank accession no. AF097923), and the characterization of its encoded protein.

MATERIALS AND METHODS

Cloning and expression of *P. falciparum* SAMS (*PfSAMS*)

A partial clone (~ 600 bp) of *PfSAMS* cDNA was initially obtained as a product of a differential analysis of cDNAs between sialic acid-dependent and sialic acid-independent populations of *P. falciparum*. Sequence analysis suggested that this clone may encode *PfSAMS*, and it was subsequently shown that this gene was not differentially expressed.

The 5′ coding region was established by two rounds of PCR using the *P. falciparum* 3D7 strain cDNA library constructed from gametocyte poly(A)$^+$ RNA, cloned into the Gibco/BRL pSPORT vector (kindly supplied by Thomas Templeton, Laboratory of Parasitic Diseases, NIAID, NIH, U.S.A.). The sense

Abbreviations used: AdoMet, S-adenosylmethionine; SAMS, AdoMet synthetase.

[1] To whom correspondence should be addressed at Division of Experimental Therapeutics, Walter Reed Army Institute of Research, Washington, DC 20307-5100, U.S.A. (e-mail peter.chiang@na.amedd.army.mil).

and antisense primers for the first PCR were: 5′-GTAAAACGACGGCCAGT-3′ (M13), and 5′-TACTAAGACACGTCTACA-3′ (nucleotides 919–936 of *PfSAMS*). The DNA fragment generated was used for the second PCR with the following sense and antisense primers: 5′-ATTTAGGTGACACTATAGAA-3′ (SP6), and 5′-CTTTGTAGTTATTTCTCC-3′ (nucleotides 184–201 of *PfSAMS*). PCR conditions were as follows: 94 °C for 2 min; followed by 30 cycles of 94 °C for 30 s, 48 °C for 30 s, and 65 °C for 2 min; final extension was at 72 °C for 7 min. After purifying the PCR products by QIAquick-spin PCR Purification Kit (QIAGEN), sequencing of the DNA was performed with an ABI Model 310 automatic sequencer. The 3′ region of the PfSAMS cDNA was cloned using the 3′ rapid amplification of cDNA ends system (Life Technologies, Rockville, MD, U.S.A.).

The full-length *PfSAMS* gene was then isolated by PCR amplification using genomic DNA from *P. falciparum* clone 3D7 as a template. The sense and antisense primers were: 5′-ATGAGTCAGTTGAAAATTAAA-3′ and 5′-TTAATTTTTTTCGTC-3′, containing nucleotides 1–21 and 1209–1195 of *P. falciparum* coding sequence, respectively. The amplified fragment was cloned into the pCR2.1 TOPO vector (Invitrogen) and sequenced on both strands. The *PfSAMS* cDNA and gene contain identical sequences, indicating that this gene contains no introns.

The 1.2 kb *PfSAMS* gene was subcloned into the pQE30 bacterial expression vector (QIAexpress System, QIAGEN) and recombinant protein was produced as previously described [21]. Briefly, M15 bacterial transformed with *PfSAMS* or human *SAMS* cDNA in the pQE30 vector was grown at 37 °C and induced by the addition of 2 mM isopropyl thio-β-galactoside (IPTG). After an additional 3.5 h of growth, the bacteria were harvested and resuspended in a one-fifth volume of a sonication buffer containing 50 mM sodium phosphate buffer, pH 7.8, containing 300 mM NaCl, 1 mg/ml lysozyme and 1 mM PMSF. After sonication and removal of cell debris, the bacterial extracts were stored frozen in 20 % (w/v) glycerol. The *PfSAMS* gene was also inserted into the pET32 vector and expressed in BLR(DE3) cells (Novagen) as a His-Tag protein, which was purified by metal chelate chromatography.

Assay of SAMS activity

SAMS activity was assayed essentially as described elsewhere [21,22]. Briefly, bacterial extracts were incubated for 30 min at 37 °C in a reaction mixture (100 μl) containing 0.1 M Tris/HCl, pH 8.2, 20 mM $MgCl_2$, 150 mM KCl, 10 mM ATP, 5 mM 2-mercaptoethanL, and 500 μM L-[*methyl*-^{3}H]methionine (0.5 μ-Ci/reaction). The reaction was stopped with 10 μl of 2 M $HClO_4$ containing 5 mM methionine. After centrifugation, 50 μl of the supernatant solution was spotted on to a phosphocellulose circle, washed in 5 mM methionine/1 % casein, dried, and measured in a scintillation counter. Each data point was determined in triplicate and presented as the mean.

Chromosomal localization and Southern blot analysis of *PfSAMS*

The location of *PfSAMS* was determined as described by pulse-field gel-assisted PCR reaction analysis (PFG-PCR) [23]. *P. falciparum* chromosomes from the FCR3 or XP5 strain were separated into 12 bands by pulsed-field gel electrophoresis using the CHEFII system (Bio-Rad Laboratories, Hercules, CA, U.S.A.) at 90 V for 120 h with switching intervals of 300–1000 s over 120 h (in 0.75 % TBE; 1 × TBE = 10.8 g Tris, 5.5 g boric acid, 0.74 g disodium EDTA·$2H_2O$). Each band was used as a template for PCR amplification of the *PfSAMS* gene, using a pair of sense (5′-TTATTCACATCTGAATCAGT-3′) and antisense (5′-TTGTGTAACCAATACTACTA-3′) primers. The PCR cycles were: 94 °C for 2 min; followed by 30 cycles of 94 °C for 10 s, 50 °C for 10 s, and 45 °C for 10 s; final extension was at 60 °C for 30 s.

P. falciparum genomic DNA was digested with *Apa*I, *Dra*I, *Cla*I, *Bcl*II, *Bgl*I, *Sau*3AI, *Hin*cII, *Msp*I, *Acc*I, *Hin*dIII, *Xba*I, *Hpa*I, or *Fok*I, electrophoresed through 0.8 % agarose gel, and transferred to a Nytran membrane. The filter was hybridized to a full-length *PfSAMS* cDNA probe labelled by random priming.

Molecular modelling

The Quanta97 package (MSI, San Diego, CA, U.S.A.) and a Silicon Graphics Octane workstation were used to model PfSAMS from the crystal structure of *E. coli* SAMS (1MXB; Protein Data Bank, Brookhaven, NY, U.S.A.). The CLUSTALW alignment was modified manually based on the secondary structure of the template protein. The side chains of residues not conserved between the *E. coli* SAMS and the PfSAMS sequences were placed using a bump search. The molecular surface of PfSAMS was visualized using the GRASP program [24].

Sequence alignment and phylogenetic analysis

The phylogenetic tree of SAMS enzymes was constructed using the neighbour-joining and protein parsimony methods with bootstrap analysis (1000 iterations) as implemented in the PHYLIP package [25]. The representative animal, plant, and bacterial sequences were extracted from the GenBank protein database and aligned using the CLUSTALW program [26]. The multiple alignment was then corrected in accordance to the PSI-BLAST [27] outputs and manually edited to remove large inserts and ambiguously aligned regions. The final alignment contained 27 sequences of 360 residues each. First, a set of 1000 distance matrices was generated using the PROTDIST program with the 'Dayhoff PAM distance' option. The distance matrices were then analysed using the protein parsimony [28] and neighbour-joining [29] methods. Consensus trees and bootstrap support for each method were calculated separately and the branches with different branching orders in the trees produced by the two methods were collapsed. Nodes that were strongly supported by bootstrap analysis (> 70 %) under both of these methods were considered reliable and were marked with dots in the Figure. Branch lengths for the derived consensus tree were computed using the Fitch–Margoliash method [30].

RESULTS

The amino acid sequence of PfSAMS is shown in Figure 1. The *PfSAMS* gene consists of 1209 bp coding for a protein of 402 amino acids with a calculated mass of 44844 Da and pI of 6.28. The gene has no introns, and has an overall base composition of 67 % A+T content, which are characteristic of other *P. falciparum* genes [31]. The recombinant PfSAMS expressed as a His-Tag protein had an apparent molecular mass of 45 kDa based on SDS/PAGE, in agreement with the expected molecular mass (results not shown).

When the sequence of PfSAMS was aligned with those of human hepatic and *E. coli* SAMS (Figure 1), it is apparent that PfSAMS retains all of the active-site amino acids involved in the binding of ADP, P_i and metal ions as do human hepatic SAMS and *E. coli* SAMS [32,33]. It has the same conserved nonapeptide P-loop for the phosphate-binding region, GGGAFSGKD [33], corresponding to residues 274–282 of PfSAMS (Figure 1). This

```
PfSAMS          -------MSQLKIKRGNFLFTSESVNEGHPDKICDQISDAILDSCLREDPYSKVACEVCA 53
H.sapiens       MNGPVDGLCDHSLSEGVFMFTSESVGEGHPDKICDQISDAVLDAHLKQDPNAKVACETVC 60
E.coli          --------------MAKHLFTSESVSEGHPDKIADQISDAVLDAILEQDPKARVACETYV 46
                             . .:******.*******.******:**: *.:** ::****.

PfSAMS          KKNYIFIFGEITTKAKVNYDKVTRDVLKHIGYDDESKGLDYKTAEIKVSIDEQSPDIAQC 113
H.sapiens       KTGMVLLCGEITSMAMVDYQRVVRDTIKHIGYDDSAKGFDFKTCNVLVALEQQSPDIAQC 120
E.coli          KTGMVLVGGEITTSAWVDIEEITRNTVREIGYVHSDMGFDANSCAVLSAIGKQSPDINQG 106
                *.. ::: ****: * *: :.:.*:.::.*** ..  *:* ::. :  :: :***** *

PfSAMS          VHENRSPELIGAGDQGIMFGYATDETENYMPLTHHYATLLGKRLTEVRKLGILPYLGPDG 173
H.sapiens       VHLDRNEEDVGAGDQGLMFGYATDETEECMPLTIILAHKLNARMADLRRSGLLPWLRPDS 180
E.coli          VDR-ADPLEQGAGDQGLMFGYATNETDVLMPAPITYAHRLVQRQAEVRKNGTLPWLRPDA 165
                *.   .    ******:******:**:  ** .   *  *  * :::*: * **:* **.

PfSAMS          KTQITIEYKNKGSCGGHLEPLRVHTVLISTQHAEDIKYEQLKTDLMENVIKYVIPEKLLD 233
H.sapiens       KTQVTVQYMQDNGA---VIPVRIHTIVISVQHNEDITLEEMRRALKEQVIRAVVPAKYLD 237
E.coli          KSQVTFQYDDGK-------IVGIDAVVLSTQHSEEIDQKSLQEAVMEEIIKPILPAEWLT 218
                *:*:*.:* :          : :.::::*.** *:*  :.::  : *::*: ::* : *

PfSAMS          NETLYYLNPSGKFVLGGPAADAGLTGRKIICDTYGGWGAHGGGAFSGKDASKVDRSAAYY 293
H.sapiens       EDTVYHLQPSGRFVIGGPQGDAGVTGRKIIVDTYGGWGAHGGGAFSGKDYTKVDRSAAYA 297
E.coli          SATKFFINPTGRFVIGGPMGDCGLTGRKIIVDTYGGMARHGGGAFSGKDPSKVDRSAAYA 278
                . * :.::*:*:**:*** .*.*:****** ***** . ********** :********

PfSAMS          LRFIAKSLVANKFCRRVLVQASYSIGIANPISLNVNSYGTVSTGYTDYDLEQIILRNFDL 353
H.sapiens       ARWVAKSLVKAGLCRRVLVQVSYAIGVAEPLSISIFTYGTSQK--TERELLDVVHKNFDL 355
E.coli          ARYVAKNIVAAGLADRCEIQVSYAIGVAEPTSIMVETFGTEKV--PSEQLTLLVREFFDL 336
                 *::**.:*   :. *  :*.**:**:*:* *: : ::** .   .. :*  :: . ***

PfSAMS          RPGFIIQELKLTEPVFSKTSAYGHFGREGDTFTWEKIKDLSHEKNALKN- 402
H.sapiens       RPGVIVRDLDLKKPIYQKTACYGHFGRS--EFPWEVPRKLVF-------- 395
E.coli          RPYGLIQMLDLLHPIYKETAAYGHFGRE--HFPWEKTDKAQLLRDAAGLK 384
                **  ::: *.* .*::.:*:.******.   *.**   .
```

Figure 1 Alignment of the amino acid sequences of PfSAMS, human hepatic (*Homo sapiens*) SAMS and *E. coli* SAMS

Active-site amino acids as projected for *E. coli* SAMS [33] are in bold. The signature sequence motif, GAGDQG, is in the first shaded box, and the phosphate-binding P-loop is in the second shaded box.

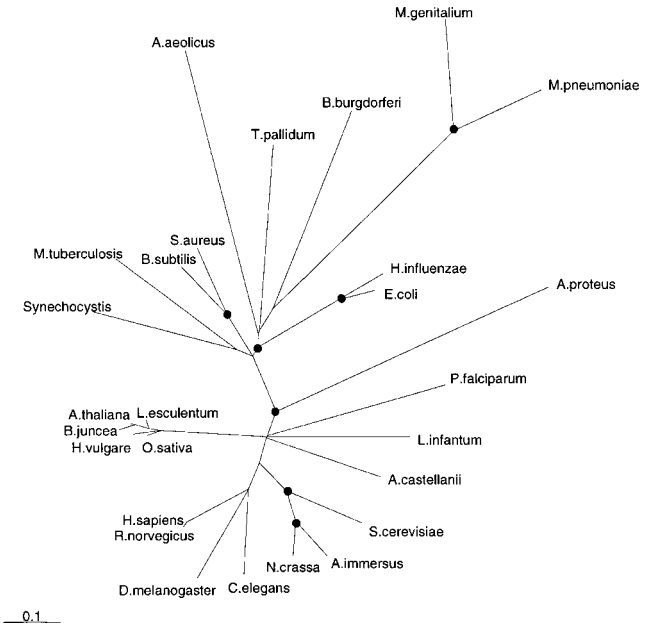

Figure 2 Cladogram for the phylogenetic relationship of SAMS proteins

The consensus phylogenetic tree was constructed using protein parsimony [24] neighbour-joining [29] methods. Dots indicate the nodes that were strongly supported by bootstrap analysis (> 70%) under both of these methods. The *P. falciparum* SAMS is from Figure 1. The source organisms for other SAMS sequences and their respective GenBank accession numbers were as follows: *Acanthamoeba castellanii,* X79205; *Amoeba proteus,* U91602; *Arabidopsis thaliana,* M33217; *Ascobolus immersus,* U21548; *Aquifex aeolicus,* AE000726; *Bacillus subtilis,* AF008220; *Borrelia burgdorferi,* AE001143; *Brassica juncea,* X80362; *Caenorhabditis elegans,* U41009; *Drosophila melanogaster,* X77392; *Escherichia coli,* AE000377; *Haemophilus influenzae,* U32797; *Homo sapiens,* X68836; *Hordeum vulgare,* D63835; *Leishmania infantum,* AF031902; *Lycopersicum esculentum,* Z24742; *Mycobacterium tuberculosis,* Z80108; *Mycoplasma genitalium,* U39684; *Mycoplasma pneumoniae,* AE000011; *Neurospora crassa,* U21547; *Oryza sativa,* U8233; *Rattus norvegicus,* AB000717; *Saccharomyces cerevisiae,* U17246; *Staphylococcus aureus,* U36379; *Synechocystis sp.,* D90901; *Treponema pallidum,* AE001250.

P-loop motif forms a binding cavity for the Mg^{2+}-ATP complex. The second signature hexapeptide for the SAMS family, GAGDQG, is also conserved in PfSAMS (residues 124–129). This is a consensus pattern, GAGDQG-x(3)-GYA, and appears in almost all SAMS of other species.

A cladogram for the phylogenetic relationship of the SAMS members from different species was constructed (Figure 2). The malarial enzyme PfSAMS is immediately related to the protozoan SAMS of *Amoeba proteus*, *Leishmania infantum* and *Amoeba castellani*. PfSAMS may also be closely related to the SAMS of plants, and appears to be phylogenetically distinct from the SAMS of bacteria, fungi and metazoa.

A three-dimensional model of PfSAMS (Figure 3) was constructed by utilizing the X-ray crystallography data (1MXB) of *E. coli* SAMS (46% identical) [33] as a template. Homodimers of *E. coli* SAMS bind two ATP molecules in the interdomain interface. Two Mg^{2+} ions and one K^+ ion also bind in each of the ATP-binding sites, and a single K^+ ion binds in a symmetry-related position in the dimer interface. The residues within 5 Å of the ATP/Mg^{2+} molecules are 88% identical between *E. coli* SAMS and PfSAMS and the residues within 3.5 Å are 100% identical. The high level of sequence conservation in the ATP/Mg^{2+} binding sites produces a surface charge distribution in PfSAMS that is very similar to the distribution found in *E. coli* SAMS, and indicates that both enzymes are likely to bind ATP/Mg^{2+} in the same manner. Figure 3(a) shows the surface-charge distribution of two PfSAMS monomers that have been rotated away from each other to expose the dimer interface. The surface in contact with the ATP phosphates is highly positively charged to stabilize the binding of the negatively charged phosphates. Similarly, two surfaces of negative charge (one from each monomer) contact the positively charged Mg^{2+} ions, and help to stabilize the ATP/Mg^{2+} complex as described for *E. coli* SAMS [33].

The K^+ ions may have a role in ATP binding as well, even though they are more than 6 Å from any part of the ATP/Mg^{2+} molecules. If the K^+ ions were not considered part of the SAMS protein and were removed from the surface-charge calculations, the positively charged surface becomes markedly more neutral, and the ATP-binding site becomes dominated by negative charge. Interestingly, all of the residues within 3.5 Å of the K^+ ions are 100% conserved between PfSAMS and *E. coli* SAMS.

PfSAMS could form dimers in a manner almost identical to that seen in *E. coli* SAMS, but PfSAMS cannot form homo-tetramers as seen in *E. coli* SAMS [34]. Figure 3(b) shows the degree of amino acid conservation between *E. coli* SAMS and PfSAMS for residues in the dimer interface. Interface residues that are identical between the two enzymes are coloured blue, while similar residues are coloured magenta. Dissimilar residues are coloured red. The two areas of dissimilar residues [labelled (A) and (B) in Figure 3b] are complementary in the sense that area (A) from one monomer will interact with area (A) from the other monomer when the dimer forms. The high degree of amino acid conservation (76% identical) in the dimer interface, and the apparent complementarity of dissimilar residues, indicates that PfSAMS forms dimers along this surface. The interface which joins pairs of dimers to form tetramers in the *E. coli* enzyme is much less extensive (12 residues from each monomer contribute to the tetramer interface versus 42 residues from each monomer for the dimer interface). In contrast to the high level of amino acid conservation seen in the dimer interface, none of the residues

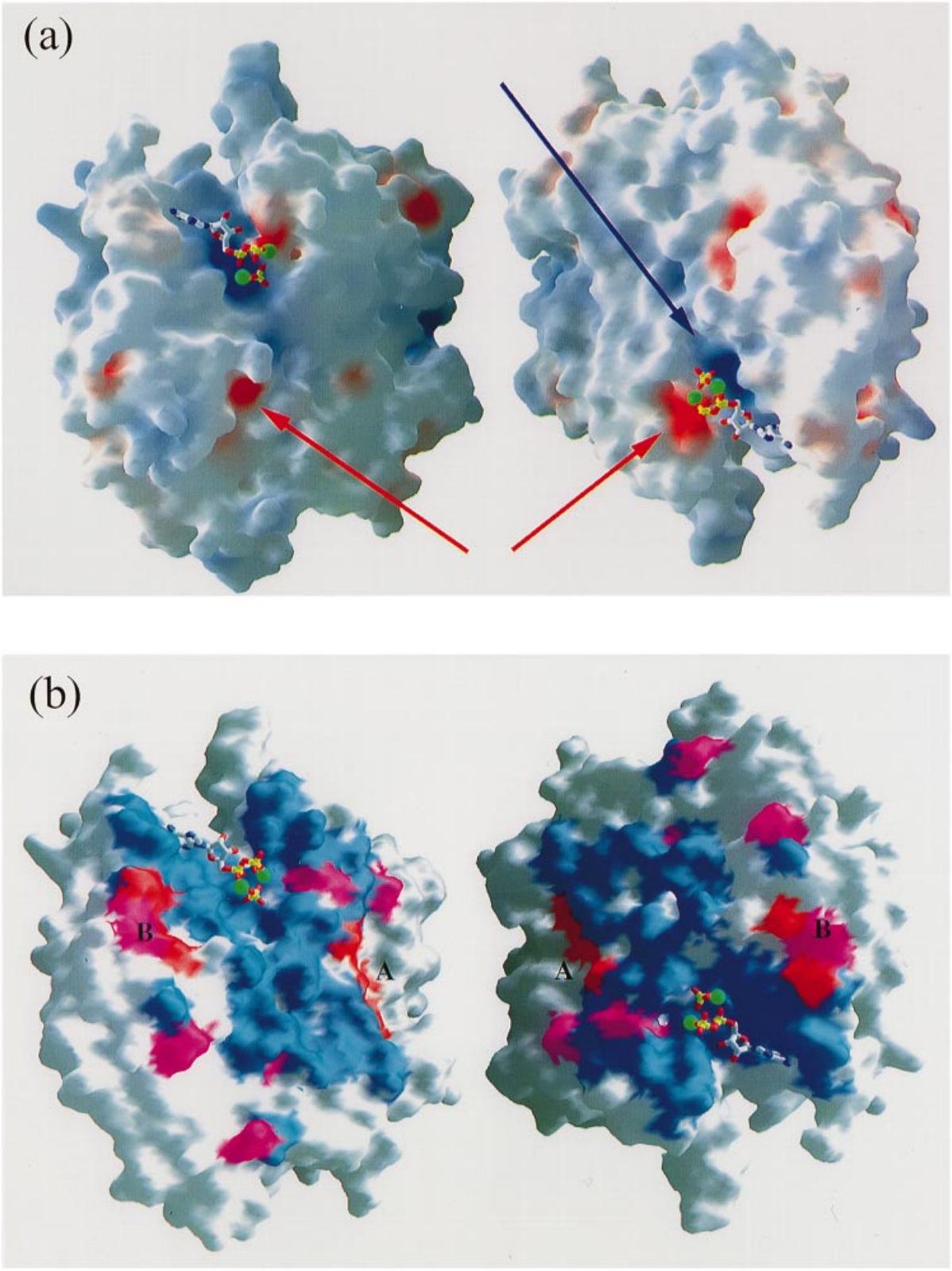

Figure 3 Molecular modelling of PfSAMS using the X-ray crystallography data of *E. coli* SAMS (1MXB) [32] as a template

(**a**) Electrostatic molecular surface of the *P. falciparum* SAMS homology model. This view exposes the PfSAMS dimer interface by rotating both monomers by 60° in opposite directions about an axis vertical in the plane of the page. Grey surface indicates uncharged areas, while blue and red indicate areas of positive and negative charge, respectively. Substrate ATP is shown coloured by atom type (carbon is grey, oxygen is red, nitrogen is blue, phosphorus is yellow) with two bound magnesium ions (green spheres) as is found in the *E. coli* SAMS structure. The ATP phosphates interact with a very positively charged surface indicated with the blue arrow. The bound magnesium ions (Mg^{2+}) interact with regions of negative charge from both monomers, indicated with the

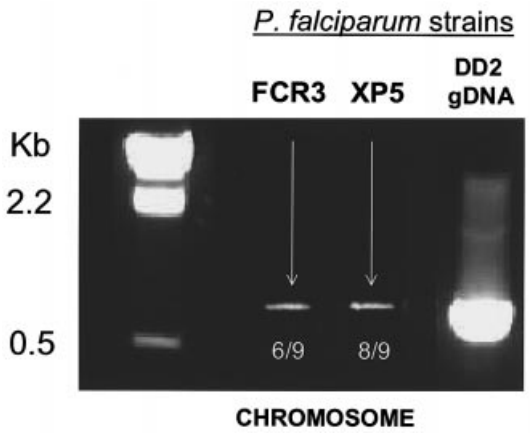

Figure 4 Chromosomal location of the gene *PfSAMS*

After pulse-field gel electrophoresis of the *P. falciparum* chromosomes from the FCR3 or XP5 strain, each gel band was used as a template for PCR as described in the Materials and methods section.

that form the *E. coli* tetramer interface are conserved in PfSAMS. Thus, it is likely that PfSAMS exists as a dimer.

Chromosomal hybridization of the FCR3 strain of *P. falciparum* chromosomes showed that *PfSAMS* is located in a band containing both chromosomes 6 and 9 (Figure 4). Since, in a similar experiment performed with the chromosomes of the XP5 strain, *PfSAMS* is located in a band containing both chromosomes 8 and 9, it is likely that the *PfSAMS* gene is in chromosome 9 of *P. falciparum* (Figure 4). Southern blot analysis of genomic DNA digested with 13 restriction enzymes indicated that *PfSAMS* is probably a single copy gene (results not shown).

The classical inhibitor of SAMS, cycloleucine [35], was used as a prototype drug to see whether there was a differential sensitivity toward inhibition between PfSAMS and the human hepatic SAMS. As shown in Figure 5, cycloleucine is a competitive inhibitor with K_i values of 17 and 10 mM for PfSAMS and hepatic SAMS, respectively.

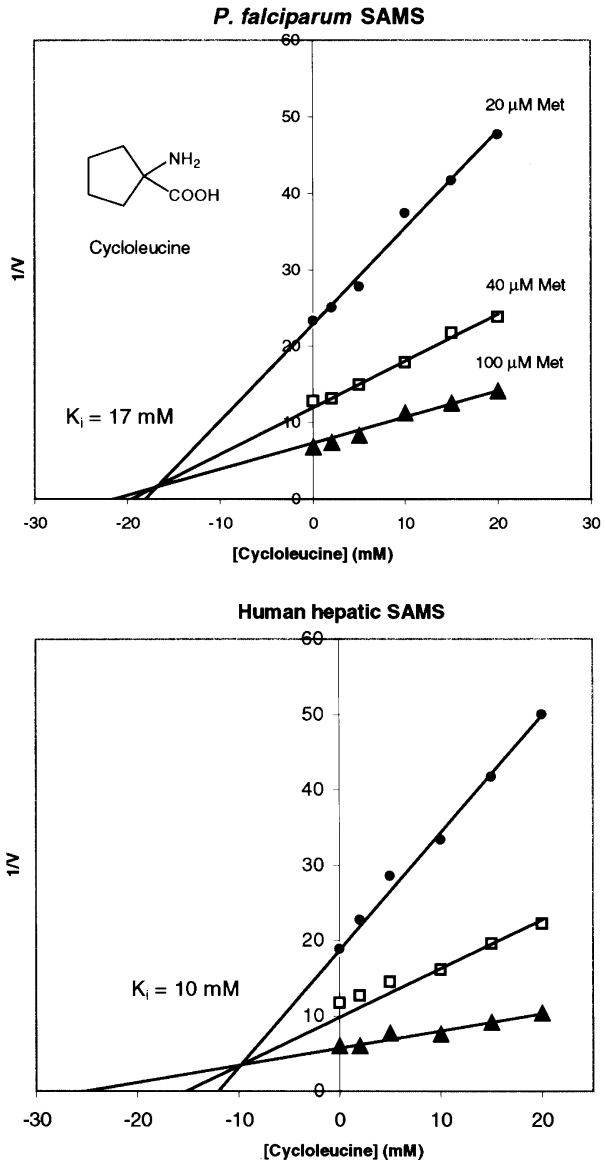

Figure 5 K_i values for the inhibition of PfSAMS and human hepatic SAMS by cycloleucine as determined by the Dixon plots

DISCUSSION

Multiple forms of *SAMS* genes and SAMS isoenzymes exist within species of divergent organisms [2,8–11]. Nonetheless, cloned PfSAMS showed remarkably conserved homology with other SAMS enzymes, both in terms of sequence and molecular mass. For example, rat kidney *SAMS* cDNA codes for 395 amino acids with a mass of 43.7 kDa [36]; *Acanthamoeba SAMS* cDNA codes 388 amino acids with a mass of 44 kDa [37]; and *Met*K of *E. coli* codes for a 42 kDa SAMS protein [38]. Southern blot analysis of *P. falciparum* genomic DNA digested with 13 restriction enzymes revealed that *PfSAMS* is probably a single copy gene. This has also been demonstrated for *SAMS* from *Drosophila melanogaster* [39], but is not the case in all species. Three *SAMS* genes in *Cantharanthus roseus* code for three SAMS isoenzymes of approx. 43 kDa [40], whereas rice (*Oryza sativa*) has two genes, which code for two SAMS, pOS-SAMS1 (43.2 kDa) and pOS-SAMS2 (42.9 kDa) [41].

PfSAMS shares highly conserved sequence similarity with other SAMS family members. The two traditional signature motifs, GAGDQG, and GGGAFSGKD, are eminently conserved in PfSAMS. The last motif is the phosphate-binding P-loop, archetypal of nucleotide-binding proteins, which share a glycine-rich region, GXXXGK[S/T] [32,33]. All the active-site amino acids for the binding of ADP, P_i and metal ions are surprisingly well preserved, exactly the same as those of human hepatic SAMS and *E. coli* SAMS [33].

red arrows. (**b**) Molecular surface of the *P. falciparum* SAMS homology model coloured by amino acid homology to *E. coli* SAMS. This orientation of the PfSAMS monomers is the same as described in (**a**) above. The molecular surface is coloured grey if the underlying residue is not within 3.5 Å of ATP/Mg^{2+} or the other monomer. The surfaces corresponding to residues in the dimer interface are coloured based on the degree of amino acid homology between *P. falciparum* SAMS and *E. coli* SAMS. Identical residues are coloured blue, similar residues are coloured magenta and dissimilar residues are coloured red. Two areas of dissimilar residues (red) are complementary such that the area labelled 'A' in one monomer will interact with the corresponding area labelled 'A' in the other monomer. Likewise, the areas labelled 'B' from both monomers will interact in the dimer interface.

It could be surmised here that PfSAMS evolved from the prokaryote SAMS into a family encompassing protozoan SAMS (Figure 2). The malarial enzyme PfSAMS is immediately related to the SAMS of other protozoans, *Amoeba proteus*, *Leishmania infantum* and *Acanthamoeba castellanii*; but appears to be distinct from the SAMS of bacteria, fungi, and metazoa.

The availability of malarial and human SAMS enzymes will allow for the rational approach towards designing antimalarial drug candidates. In this regard, we have begun the initial evaluation of compounds known to inhibit SAMS. Even though the human enzyme is about twofold more sensitive to the inhibition by cycloleucine than the malarial enzyme, it appears that methionine analogues may not be the drugs of choice to develop an antimalarial therapy because of the poor K_i values (Figure 5). However, the development of techniques such as antisense technology for the targeting of genomic sequences will allow the use of malarial genes as molecular targets [42].

It remains to be established whether *PfSAMS* is differentially expressed during the life cycle of *P. falciparum*. For example, the two rice *SAMS* genes are regulated in a tissue-specific manner or environmentally, but their expression is coordinated during growth [41]. The induction of SAMS in T-lymphocytes by interleukin-2 is cell-cycle-dependent [43]. Similarly, when *Acanthamoeba* converts into the cyst state, there is a pronounced reduction in the level of *SAMS* transcripts [37]. Therefore, the study of *PfSAMS* during the different life-cycle stages of *P. falciparum* should prove to be interesting, and may shed light on its virulence and why it is the most malignant of all human malarial parasites.

REFERENCES

1 Cantoni, G. L. (1953) J. Biol. Chem. **204**, 403–416
2 Chiang, P. K. and Cantoni, G. L. (1977) J. Biol. Chem. **252**, 4506–4513
3 Kotb, M. and Geller, A. M. (1993) Pharmacol. Ther. **59**, 125–143
4 Tabor, C. W. and Tabor, H. (1984) Adv. Enzymol. **56**, 251–282
5 Chiang, P. K., Gordon, R. K., Tal, J., Zeng, G. C., Doctor, B. P., Pardhasaradhi, K. and McCann, P. P. (1996) FASEB J. **10**, 471–480
6 Chiang, P. K. (1998) Pharmacol. Ther. **77**, 115–134
7 Lomardini, J. B. and Talalay, P. (1973) Mol. Pharmacol. **9**, 542–560
8 Kotb, M., Mudd, S. H., Mato, J. M., Geller, A. M., Kredich, N. M., Chou, J. Y. and Cantoni, G. L. (1996) Trends Genet. **13**, 51–52
9 Thomas, D. and Surdin-Kerjan, Y. (1997) Microbiol. Mol. Biol. Rev. **61**, 503–532
10 Satishchandran, C., Taylor, J. C. and Markham, G. D. (1993) Mol. Microbiol. **9**, 835–846
11 Hoffman, J. L. (1994) Adv. Pharmacol. **27**, 449–477
12 Su, X.-Z. and Wellems, T. E. (1998) in Malaria: Parasite Biology, Pathogenesis, and Protection (Sherman, I. W., ed.), pp. 253–266, ASM Press, Washington, D.C.
13 Miller, L. H. and Smith, J. D. (1998) Nature Med. **4**, 1244–1245
14 Gardner, M. J., Tettelin, H., Carucci, D. J., et al. (1998) Science **282**, 1126–1132
15 Bender, C. M., Zingg, J. M. and Jones, P. A. (1988) Pharm. Res. **15**, 175–187
16 Szyf, M. (1996) Pharmacol. Ther. **70**, 1–37
17 Trager, W., Tershakovec, M., Chiang, P. K. and Cantoni, G. L. (1980) Exp. Parasitol. **50**, 83–89
18 Whaun, J. M., Miura, G. A., Brown, N. D., Gordon, R. K. and Chiang, P. K. (1986) J. Pharmacol. Exp. Ther. **236**, 277–283
19 Bitonti, A. J., Baumann, R. J., Jarvi, E. T., McCarthy, J. R. and McCann, P. P. (1990) Biochem. Pharmacol. **40**, 601–608
20 Mayers, D. L., Mikovits, J. A., Joshi, B., et al. (1995) Proc. Natl. Acad. Sci. U.S.A. **92**, 215–219
21 Chamberlin, M. E., Ubagai, T., Mudd, S. H., Wilson, W. G., Leonard, J. V. and Chou, J. Y. (1996) J. Clin. Invest. **98**, 1021–1027
22 Ubagai, T., Lei, K.-J., Huang, S., Mudd, S. H., Levy, H. J. and Chou, J. Y. (1995) J. Clin. Invest. **96**, 1943–1947
23 Su, X.-Z. and Wellems, T. E. (1999) Exp. Parasitol. **91**, 367–369
24 Nicholls, A. (1993) GRASP: graphical representation and analysis of surface properties, Columbia University Press, New York, U.S.A.
25 Felsenstein, J. (1996) Methods Enzymol. **266**, 418–427
26 Thompson, J. D., Higgins, D. G. and Gibson, T. J. (1994) Nucleic Acids Res. **22**, 4673–4680
27 Altschul, S. F., Madden, T. L., Schaffer, A. A., Zhang, J., Zheng, Z., Miller, W and Lipman, D. J. (1997) Nucleic Acids Res. **25**, 3389–3402
28 Felsenstein, J. (1988) Annu. Rev. Genet. **22**, 521–565
29 Saitou, N. and Nei, M. (1987) Mol. Biol. Evol. **4**, 406–425
30 Fitch, W. M. and Margoliash, E. (1967) Science **155**, 279–284
31 Su, X.-Z. and Wellems, T. E. (1996) Nucleic Acids Res. **24**, 1574–1575
32 Saraste, M., Sibbald, P. R. and Wittinghofer, A. (1990) Trends Biochem. Sci. **15**, 431–434
33 Takusagawa, F., Kamitori, S. and Markham, G. D. (1996) Biochemistry **35**, 2586–2596
34 Markham, G., Hafner, E., Tabor, C. and Tabor, H. (1980) J. Biol. Chem. **255**, 9082–9092
35 Sufrin, J. R., Coulter, A. W. and Talalay, P. (1979) Mol. Pharmacol. **15**, 661–677
36 Horikawa, S., Sasuga, J., Shimizu, K., Ozasa, H. and Tsukada, K. (1990) J. Biol. Chem. **265**, 13683–13686
37 Ahn, K.-S. and Henry, Jr., H. (1997) Biochim. Biophys. Acta **1351**, 223–230
38 Markham, G. D., DeParasis, J. and Gatmaitan, J. (1984) J. Biol. Chem. **259**, 14505–14507
39 Larsson, J. and Rasmuson-Lestander, Å. (1994) FEBS Lett. **342**, 329–333
40 Schröder, G., Eichel, J., Breinig, S. and Schröder, J. (1997) Plant Mol. Biol. **33**, 211–222
41 Lee, J.-H., Chae, H. S., Lee, J.-H., Hwang, B., Hahn, K. W., Kang, B. G. and Kim, W. T. (1997) Biochim. Biophys. Acta **34**, 13–18
42 Milhous, W. K. and Kyle, D. E. (1998) In Malaria: Parasite Biology, Pathogenesis, and Protection, (Sherman, I. W., ed.), pp. 303–316, ASM Press, Washington, D.C.
43 Tobeña, R., Horikawa, S., Calvo, V. and Alemany, S. (1996) Biochem. J. **319**, 929–933

Received 10 June 1999/2 August 1999; accepted 2 September 1999